

Removal of polycyclic aromatic hydrocarbons (PAHs) from groundwater by heterogeneous photocatalysis under natural sunlight

Nuria Vela^a, Marina Martínez-Menchón^b, Ginés Navarro^b, Gabriel Pérez-Lucas^b, Simón Navarro^{b,*}

^a Facultad de Enfermería, Universidad Católica San Antonio de Murcia, Campus de Los Jerónimos, s/n. Guadalupe, 30107, Murcia, Spain

^b Departamento de Química Agrícola, Geología y Edafología, Facultad de Química, Universidad de Murcia, Campus Universitario de Espinardo, 30100, Murcia, Spain

ARTICLE INFO

Article history:

Received 23 December 2011
Received in revised form 25 January 2012
Accepted 4 February 2012
Available online 11 February 2012

Keywords:

Groundwater
Photodegradation
Polycyclic aromatic hydrocarbons
Titanium dioxide
Zinc oxide

ABSTRACT

Polycyclic aromatic hydrocarbons (PAHs) are a class of persistent organic pollutants of special concern because they are carcinogenic and mutagenic compounds. In this paper, photodegradation of a mixture of six PAHs in groundwater at pilot plant scale is reported. Semiconductor materials (ZnO and TiO₂) as photocatalysts in tandem with Na₂S₂O₈ as oxidant under natural sunlight were used. The PAHs were benzo[*a*]pyrene, benzo[*b*]fluoranthene, benzo[*ghi*]perylene, benzo[*k*]fluoranthene, fluoranthene, and indene[1,2,3-*cd*]pyrene. As expected, the influence of both semiconductors on the degradation of PAHs was very significant in all cases. Photocatalytic experiments show that the addition of photocatalyst, especially for ZnO/Na₂S₂O₈ system, strongly improves the elimination of PAHs in comparison with photolytic tests; significantly increasing the reaction rates. The first-order equation (monophasic model) satisfactorily explained the disappearance process although it ignores small residues remaining late in the process. These residues are important from an environmental point of view and the Hoerl function (biphasic model) better predict the results obtained. In our conditions, the time required for 90% degradation was in the range 7–15 min and 18–76 min for ZnO and TiO₂ systems, respectively. Thus, the use of the tandem ZnO/Na₂S₂O₈ makes possible the economical decontamination of groundwater containing non-biodegradable pollutants like PAHs.

© 2012 Elsevier B.V. All rights reserved.

1. Introduction

Polycyclic aromatic hydrocarbons (PAHs) refer to hydrocarbons containing two or more fused benzene rings. Benzo[*a*]pyrene is one of the most studied; its high retention in the environment makes this compound is used as a reference in many environmental studies [1]. The physical and chemical properties vary depending on the molecular weight [2]. All PAHs are neutral and nonpolar compounds and they have high stability, existing a great difficulty to be degraded. All of them have high melting points and low vapor pressures and water solubilities. Generally, PAH solubility and volatility decrease and hydrophobicity increases with an increase in the number of fused benzene rings.

Because PAHs are ubiquitous contaminants in the environment, humans are exposed to these chemicals as part of every day living. They are included in the priority list of pollutants of US EPA and European Union, especially those with four or more rings, due to their toxic, mutagenic and carcinogenic potential [3]. PAHs are previously activated in the body before exerting its effect as an endocrine disruptor or carcinogenic/mutagenic affecting growth,

reproduction, the immune system and even survival of exposed organisms.

PAHs can be found in all environmental compartments, air, soil, water and biota. These compounds are generally generated by natural and anthropogenic processes and can be introduced into the environments through various routes. The main natural sources are volcanic eruptions and forest and prairie fires, which introduce PAHs into the atmosphere [4,5]. Also, fungi are proposed to be the major precursor carriers for perylene in sediments [6].

There are two types of anthropogenic sources of PAHs: petrogenic and pyrogenic sources. Petrogenic sources tend to be oil spills from crude and refined petroleum, introduced to aquatic environments through accidental, discharge from routine tanker operations, municipal and urban runoff, and so on. These sources are associated with the generation of high molecular weight PAHs [7–9]. On the other hand, pyrogenic sources are produced by incomplete combustion of fossil fuels (coal and petroleum) and biomass at high temperatures, such as burning wood, which are released into the environment in the form of exhaust and solid residues [5,10–12]. These sources are associated with the generation of low molecular weight PAHs [13–15]. Similarly, the snuff smoke, kerosene heaters unvented heating, gas cooking and heating appliances can be important sources in indoor air [16–19]. In this context, in order to analyze the sources of pollution in aquatic ecosystems, it is

* Corresponding author. Tel.: +34 868 887477; fax: +34 868 884148.
E-mail address: snavarro@um.es (S. Navarro).

important to differentiate between surface-, ground- and drinking water.

Pollution sources in surface water are the most studied in the literature, since they represent the greatest contribution of these compounds to the aquatic environment. PAHs enter in surface waters through atmospheric deposition, surface runoff in urban centers, or industrial discharges, including oil spills. Between 10% and 80% of the input of these compounds in the oceans corresponds to atmospheric precipitation. A study shows that the total PAH inputs from the atmosphere to the western Mediterranean Sea was estimated to about 47.5 t year⁻¹, while the total PAH riverine inputs amount was 5.3–33 t year⁻¹ and 1.3 t year⁻¹ from the Rhone and Ebro rivers, respectively [20].

PAHs in groundwater can come from contamination of surface water, agricultural effluent, irrigation water, landfill leachate or contaminated soil itself. However, the movement and transport of these compounds in the soil as well as their mechanisms of groundwater penetration, remains unclear [21]. A study of carcinogenic PAH concentrations in inland waters of the United States found that their concentration in groundwater was between 0.2 and 6.9 ng L⁻¹, while in surface water was frequently in the range 2–50 ng L⁻¹ [22]. However, the concentration of these compounds in groundwater near of surface can be increased after rainy periods, demonstrating the rapid transfer of PAHs to groundwater [23]. The EU Water Framework Directive (WFD, 2000/60/EC) [24] establishes the objective of reaching good groundwater chemical and quantitative status across Europe by 2015. The directive defines “good ecological and chemical status” in terms of low levels of chemical pollution as well as a healthy ecosystem. The establishment of detailed quality criteria for the assessment of groundwater chemical status in Europe was laid down in the new Groundwater Directive (GWD, 2006/118/EC) [25]. The GWD defines groundwater as a valuable natural resource that should be protected against pollution and deterioration and considers groundwater as the most sensitive and the largest body of freshwater in the European Union and, in particular, a main source of public drinking water supplies in many regions.

The presence of PAHs in drinking water may be due to the use of natural waters contaminated by these compounds or by the use of coated pipes of coal tar in water supply systems in some countries [26]. The framework of the European legal regulations establishes health criteria for drinking water, as required by European Council Directive 98/83/EC. This directive has set a Maximum Admissible Concentration (MAC) of 0.01 µg L⁻¹ for benzo(a)pyrene and 0.1 µg L⁻¹ for the total amount of benzo(b)fluoranthene, benzo(ghi)perylene, benzo(k)fluoranthene and indene(1,2,3-cd)pyrene.

Therefore, effective, low-cost and robust methods to decontaminate waters are needed, which do not further stress the environment or endanger human health. Conventional water treatment processes are becoming less effective with the identification of more contaminants, rapid population growth increasing industrial activity and the diminishing availability of water resources. The water contaminated with PAHs can generally be processed efficiently by biological treatment plants by adsorption with activated carbon or other adsorbents, or by conventional chemical treatments (thermal oxidation, ozonation, chlorination, potassium permanganate, etc.). However, in some cases these procedures are inadequate to achieve the purity required by law.

Photolysis is one of the major transformation processes affecting the fate of PAHs in the aquatic environment. Sunlight photoalteration processes are well known to play an important role in the degradation of PAHs and other contaminants in water by generation of highly reactive intermediates, mainly hydroxyl radical (•OH), a powerful non-specific oxidant ($E^\circ = 2.8\text{ V}$). Recent advances in water purification have led to development of

oxidation processes to remove persistent organic pollutants dissolved in the aquatic environment. These methods are based on catalytic and photochemical processes to produce profound changes in the chemical structure of pollutants and they have been called Advanced Oxidation Processes (AOPs). These can be used alone or in combination with conventional methods [27].

With this aim, the objective of the present work was the application of photocatalytic processes by use of semiconductor materials (ZnO and TiO₂) for the removal of the residual concentrations of several PAHs from groundwater below the standard levels established in the Directive 98/83/EC. Previously we have studied the leaching potential of the PAHs by use of disturbed soil columns.

2. Materials and methods

2.1. Chemicals and reagents

Analytical standard PAH-Mix 3 was purchased from Dr. Ehrenstorfer GmbH (Augsburg, Germany) containing the six compounds under study (benzo[a]pyrene [BaP], benzo[b]fluoranthene [BbF], benzo[ghi]perylene [BghiP], benzo[k]fluoranthene [BkF], indene[1,2,3-cd]pyrene [InD] and fluoranthene [Fl]), at concentrations ranging from 20 to 50 µg mL⁻¹ (in acetonitrile). The main physical–chemical properties of the compounds are shown in Table 1 [28]. PAHs intermediate standard solutions were prepared by dilution in the same solvent in order to obtain the corresponding calibration and detection limits. All solvents used for sampling processing and analysis (acetonitrile, methanol and dichloromethane) were analytical grade and supplied by Scharlau (Barcelona, Spain). Deionized water (18 MΩ cm resistivity) was obtained from a Milli-Q ultrapure water purification system (Millipore, Bedford, USA).

Zinc oxide (99.9%, 10 m² g⁻¹, <70 µm), titanium dioxide (99.9%, 45 m² g⁻¹, 32 nm, anatase/rutile 88/12) were purchased from Alfa Aesar (Karlsruhe, Germany). Sodium peroxydisulfate (98%) was purchased from Panreac Química (Barcelona, Spain).

2.2. Analytical determinations

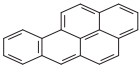
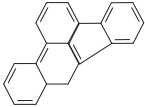

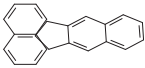
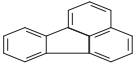
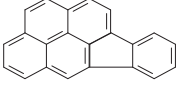
2.2.1. Sample extraction

Water samples were extracted using a solid-phase extraction (SPE) system from Supelco (Bellefonte, USA). The OASIS HLB[®] cartridges, 6 mL and 200 mg (Waters) were first conditioned with 5 mL of dichloromethane, and then washed with 5 mL of methanol followed by 5 mL of deionized water. Water samples (50 mL) were passed through the cartridges at a flow rate of 5 mL min⁻¹ under vacuum. Following extraction, the cartridges were washed with 5 mL of deionized water followed by elution with 10 mL of dichloromethane. After water was removed from the extract by anhydrous Na₂SO₄, the extracts were concentrated in a rotary evaporator in temperatures below 35 °C to a volume of ca. 1–3 mL and then under gentle stream of nitrogen. Finally, the residues were reconstituted in 1 mL of acetonitrile, filtered through 0.45 µm polytetrafluoroethylene (PTFE) filters (Millipore, Dedford, USA), transferred to 2 mL vials and kept in a freezer until analysis.

2.2.2. HPLC-FLD analysis

For analytical determination, 20 µg L⁻¹ were injected into the Alliance HPLC-FLD system, which consisted of a Waters e2695 separation module (Waters, Mildford, USA) equipped with a vacuum degasser, a quaternary pump, an autosampler and coupled to a fluorescence detector 2474 variable wavelength (Waters). Data were collected and integrated with Waters Empower[®] software. A Supelcosil[™] LC-PAH (5 cm, 4.6 mm inside diameter, 3 µm diameter particle column) with a Supelguard Discovery C18 guard column (20 mm × 4 mm inside diameter, 5 µm, Supelco, Bellefonte, USA) was used. Analyses were performed, at 290 nm and 460 nm as

Table 1
Physical–chemical characteristics of the PAHs used in this study.

PAH	Chemical structure	Molecular weight	Log K_{ow}	Water solubility (mg L^{-1})	Log K_{oc}
Benzo(a)pyrene [BaP]		252.3	6.1	1.6×10^{-3}	5.9
Benzo(b)fluoranthene [BbF]		252.3	5.8	1.5×10^{-3}	5.0
Benzo(g,h,i)perylene [BghiP]		276.6	6.6	2.6×10^{-4}	5.7
Benzo(k)fluoranthene [BkF]		252.3	6.1	8.0×10^{-4}	5.6
Fluoranthene [Fl]		202.2	5.2	2.6×10^{-1}	4.5
Indene(1,2,3-cd)pyrene [InD]		276.3	6.7	1.9×10^{-4}	6.2

excitation and emission wavelength, respectively. Separation was achieved using binary elution gradient consisting of acetonitrile (A) and water (B). The gradients were as follows: 60% of A held for 1 min, increased linearly to 100% of A during 7.5 min, held for 0.5 min, and decreased to 60% of A during 1 min to allow for equilibration before the subsequent injection.

Calibration curves were built in between 0.5 and 100 $\mu\text{g L}^{-1}$ with standard solutions containing all studied PAHs. Calibration curves were derived by least-squares regression. Equations of the calibration curves were also used to estimate the detection limits (LOD) and the quantification limits (LOQ) of each PAH. LOD and LOQ were obtained by dividing, respectively, 3 and 10 times the signal to noise ratios by the angular coefficients of the calibration curves. Signal to noise ratios were estimated by the standard deviations of peak areas obtained after 10 subsequent injections of the 0.5 $\mu\text{g L}^{-1}$ standard. To test the repeatability of the method, 10 water samples were spiked at two concentration levels (0.1 and 1.0 $\mu\text{g L}^{-1}$). To evaluate the accuracy of the method, the recoveries were determined by the standard addition technique. The calibration samples by spiking PAHs at two concentration levels (0.1 and 2.5 $\mu\text{g L}^{-1}$) into water samples were analyzed in five replicates.

2.2.3. Total organic carbon (TOC) determination

An Analyzer Shimadzu TOC Vcsh (Kyoto, Japan) provided with an NDIR detector (680 °C combustion catalytic oxidation technique) was used (LOD = 4 $\mu\text{g L}^{-1}$ and accuracy <2%).

2.3. Photocatalytic experiment

2.3.1. Solar plant

The experiment was carried out in a pilot plant in Murcia, SE Spain, latitude 38°01'15"N and longitude 1°09'56"W (UTM 30S66102420979), using natural sunlight irradiation during summer, 2010. The values (mean \pm SD) of visible plus near-infrared (400–1100 nm), UVA (315–400 nm), UVB (280–315 nm) and UVC (200–280 nm) radiation were taken with a portable photoradiometer Delta Ohm HD 2102.2 (Caseelle di Selvazzano, Italy). The mean values of VIS+NIR, UVA, UVB and UVC at 13 h were 962.2 \pm 23.6, 24.2 \pm 1.9, 1.7 \pm 0.2 and 0.2 \pm 0.1 (all in W m^{-2}), respectively.

The solar pilot plant used in this experiment is based on compound parabolic collector (CPC) technology. This small prototype consists of one photoreactor module (1.27 m^2) with five borosilicate tubes (200 cm length \times 4 cm i.d.) mounted on curved polished aluminum reflectors (0.9 cm radius of curvature) running in east-west line. The water flows directly from tube one to another connected in series and finally to the reservoir tank (250 L) and a centrifugal pump (0.55 kW) before returning (45 L min^{-1}) to the collector tubes in a closed circuit. The reaction system was continuously stirred to achieve a homogeneous suspension and thermostated by circulating water to keep the temperature at 25 \pm 2 °C. The illuminated volume was 12.5 L and the dead volume in the PVC tubes about 6 L. Storage tank, flowmeter, sensors (pH, O_2 and T), pipes, and fittings completed the installation.

2.3.2. Photocatalysis design

At the beginning of the photocatalytic test, 150 L of well water (pH = 8.06 \pm 0.07, EC = 1.12 \pm 0.11 dS m^{-1} , and TOC = 0.21 \pm 0.05 mg L^{-1}) were mixed with the analytical standard to reach a spiking level of about 2–5 $\mu\text{g L}^{-1}$ of each PAH. The respective mixtures were homogenized by shaking for 15 min to constant concentration in the dark with collectors covered by a black awning.

The photocatalysts (ZnO and TiO_2) and oxidant ($\text{Na}_2\text{S}_2\text{O}_8$) were added at 150 mg L^{-1} and the cover was removed after 15 min in order to achieve the maximum adsorption of the PAHs onto semiconductors surface. Several samples (0, 10, 20, 40, 60, 120, 240, and 480 min) were taken during the photoperiod (8 h), from 10 to 18 h. Air was periodically injected into the tank to maintain the O_2 concentration around 4–6 mg L^{-1} . A parallel blank assay, without semiconductor and $\text{Na}_2\text{S}_2\text{O}_8$ (photolysis experiment), was carried out. In all cases, assays were replicated three times.

2.4. Leaching study

2.4.1. Soil used for the leaching experiment

The silty clay loam soil selected for this study was a Hypercalcic Calcisol [29] from the Campo de Cartagena (south-eastern Spain). Soil samples were collected from the surface (top 25 cm), air-dried, and passed through 2 mm sieve. The characteristics of the soil were

as follows: sand 19.5%, silt 47.2%, clay 33.3%, organic matter 0.6%, pH 7.6.

2.4.2. Downward movement of the PAHs through the disturbed soil columns

The experiment was performed according to the OECD guidelines [30]. Downward movement of the PAHs was studied in polyvinyl chloride (PVC) columns of 40 cm (length) \times 4 cm (i.d.) packed with 200 g of soil (bulk density 1.29 g cm^{-3}). The top 3 cm of the columns were filled with sea sand and the bottom 3 cm with sea sand plus nylon mesh with an effective pore diameter of $60 \mu\text{m}$ to minimizing the dead-end volume and prevent losses of soil during the experiment. Before the application of the compounds, columns (three replications at room temperature, avoiding direct light) were conditioned with 0.01 M CaCl_2 in distilled water to their maximal water holding capacity and then allowed to drain for 24 h. The pore volume (PV) of the packed columns was estimated by the weight difference of water-saturated columns versus dry columns. The calculated PV (mL) of the soil columns after saturation was $72.7 \pm 0.5 \text{ mL}$. Following this, 1 mL of an acetonitrile/water solution (10/90, v/v) containing $20 \mu\text{g}$ of each one of the B[a]P, B[b]F, B[a]P, B[k]F, $40 \mu\text{g}$ of InD, and $50 \mu\text{g}$ of Fl, which is equivalent to a total concentration of 850 ng g^{-1} in each column (as \sum PAHs).

Twenty-four hours after PAHs application, the compounds were leached with 1000 mL of 0.01 M CaCl_2 in order to minimize soil mineral balance disruption during 10 days with a peristaltic pump. The leachates (100 mL day^{-1}) were quantitatively collected at the bottom of the columns, filtered through nylon membrane filter ($0.45 \mu\text{m}$) and extracted as previously specified. After this time, the columns were opened and the soil separated in two segments of approximately 10 cm each. Dried soil samples (5 g) were extracted with 30 mL of acetonitrile/water (2/1) by sonication. A 200 W sonic dismembrator equipped with standard titanium probe (Dr. Hielscher GmbH, Stahnsdorf, Germany) was used for sample extraction. After this, 20 mL of dichloromethane were added and then centrifuged for 10 min at $1900 \times g$. Finally, the organic phase was concentrated, reconstituted in 1 mL of acetonitrile, and analyzed by HPLC-FLD.

2.4.3. Kinetics of the photocatalytic process

Kinetics of PAHs degradation was calculated using the first-order equation:

$$C_t = C_0 e^{-kt} \quad \text{or} \quad \ln \frac{C_0}{C_t} = kt \quad (1)$$

where C_0 and C_t are the PAH concentration at times zero and t , respectively, and k the rate constant.

First-order degradation rate constants were determined by regression analysis. Half-lives ($t_{1/2}$), were calculated by replacing C by $C_0/2$ in Eq. (1), according to the following equation:

$$t_{1/2} = \ln \frac{2}{k} \quad (2)$$

This model, widely used, is usually valid when the reaction times are short. However, when the reaction is prolonged in time, it is not appropriate to explain the behavior of pollutants because the results lead to negative concentrations although acceptable values of the correlation coefficient (R^2) may be achieved. When the linear estimation fails, other equations such as those provided in two-phase models can be used with better results, especially when there is an initial rapid degradation and a subsequent phase in which the compound disappears more slowly. In some cases, a modified first-order model proposed by Hoerl [31] has been used to advantage by some authors [32]:

$$C_t = a e^{bt} t^c \quad (3)$$

or once linearized

$$\ln C_t = \ln a + bt + c \ln t \quad (4)$$

The parameters a and b are similar to C_0 and k in first-order model, and c is a measure of the deviation from exponential behavior. When $c < 0$, the function simulates a biphasic pattern [33,34]. For this model, the persistence can be estimated as the time needed to reach 50% of the initial concentration (DT_{50}).

2.5. Statistical analysis

The curve fitting and statistical data were obtained using SigmaPlot version 12.0 statistical software (Systat, Software Inc., San Jose, CA).

3. Results and discussion

3.1. Analytical determination

Calibration curves presented excellent correlation coefficients ($R^2 > 0.998$) showing the good relationship between concentration and fluorescence intensity in the studied range. LOQs were sufficiently low (0.003 – $0.132 \mu\text{g L}^{-1}$ for BkF and InD, respectively) to allow PAH determination below the MACs established for drinking and fresh water European legislation.

Recoveries were evaluated in two different levels (0.1 – $2.5 \mu\text{g L}^{-1}$). Very good recoveries (87–97%) were obtained in all cases showing the accuracy of the method and its robustness.

3.2. Preliminary studies (leaching)

The distribution from soil and water for the PAHs applied to soil columns is shown in Fig. 1. Total recoveries of PAHs from soil and water were in the range 83–112% for B[a]P and B[b]F, respectively. All PAHs were found in leachates although the amounts recovered were lower than $0.1 \mu\text{g}$ in all cases. The major fraction of all compounds was recovered from the upper soil layer (0–10 cm).

Cumulative breakthrough curves (BTCs) of the PAHs applied to disturbed soil columns are shown in Fig. 2. As can be seen, all compounds appear in the first leachate corresponding to 1.4 pore volumes (PVs) with. A substantial increment was observed when 8 PVs (600 mL) were passed. All PAHs have low leachability because the total amount leached ($0.21 \mu\text{g}$) was about 0.12% of the whole mass fraction applied to the column ($170 \mu\text{g}$). The amounts leached ranged from 10 to 60 ng from B[a]P and B[ghi]P.

According to the levels found in leachates (0.01 – $0.06 \mu\text{g L}^{-1}$), we can affirm that toxicological hazard exists because, although small, the amounts are close to the MACs set for drinking water in European Directive 98/83/EC (0.01 – $0.1 \mu\text{g L}^{-1}$).

3.3. Photolytic degradation

Fig. 3 shows the degradation of PAHs in groundwater using semiconductor materials (photocatalysis), or not (photolysis), during the studied photoperiod (480 min). PAHs may be degraded through either direct or sensitized photochemical reactions. Under sunlight, the PAHs were degraded slowly compared with the reaction rates in the presence of photocatalysts, especially ZnO. The final PAHs carryover in the photolysis experiment ranged from 23% to 67% for Fl and B[k]F, respectively. This decay of PAHs concentration could be due to direct photolysis since those compounds absorb light in the 200–400 nm range which overlaps the emission spectrum of sunlight [35].

Attempts to quantify photolytic processes are complicated by the diversity of possible transformations such as with singlet oxygen or other excited-state species, H-atom abstraction, and free

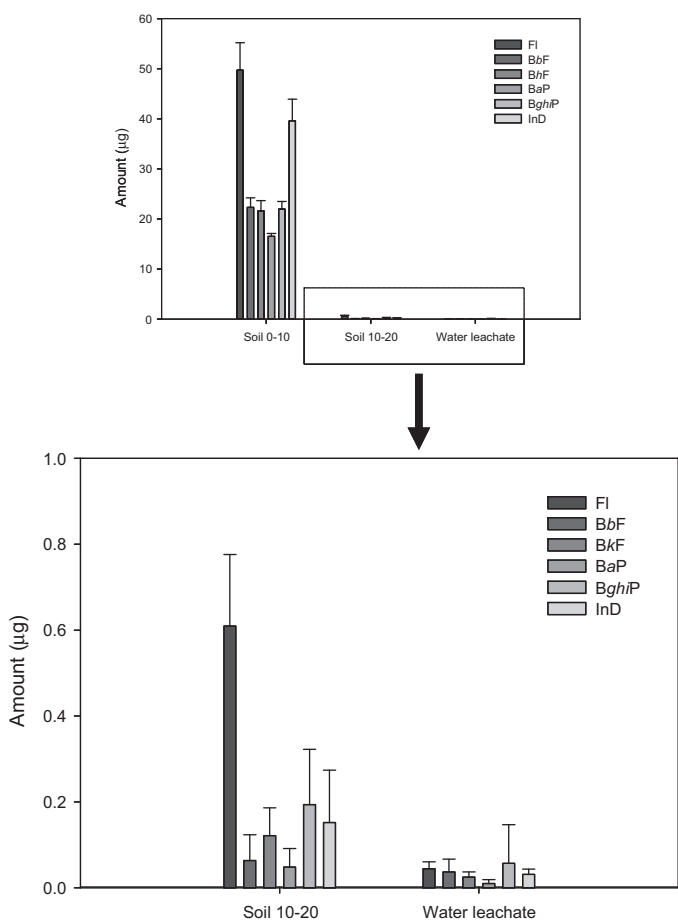


Fig. 1. Distribution of PAHs from soil and water applied to disturbed soil columns. The error bars denote standard deviation.

radical chain reactions [36]. In dilute aqueous systems, direct photolysis in which the molecule of interest absorbs light and subsequently degrades has been proposed as main responsible for the degradation of PAHs because the reactive oxygen species are not generated efficiently and are consumed rapidly in most natural waters. This degradation could be enhanced in natural waters through reactions with intermediates produced photochemically

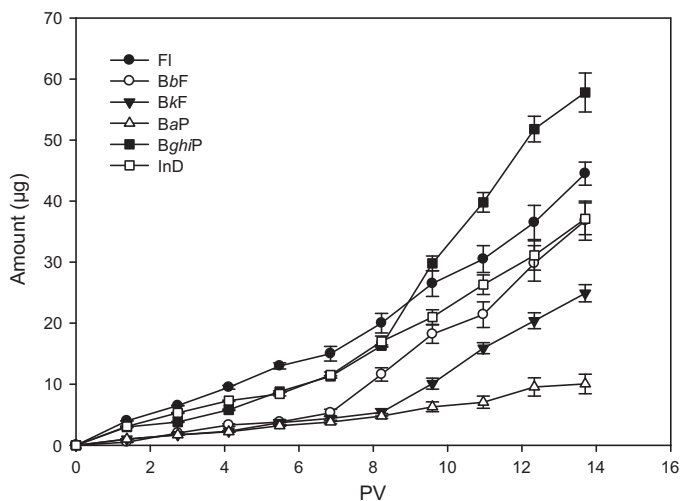


Fig. 2. Cumulative breakthrough curves (BTCs) of PAHs applied to disturbed soil columns. The error bars denote standard deviation.

from colored dissolved organic matter (CDOM) and other natural constituents such as nitrite, nitrate and some metal ions through ligand-to-metal charge-transfer reactions and photo-Fenton chemistry [37]. However, how PAHs degradation may be affected by constituents of natural waters such as DOM is still largely unknown because the photocatalytic effect of DOM described in the scientific literature is contradictory. Some authors have demonstrated that the presence of dissolved organic matter (DOM) in drinking water may act as influential factor in pollutant dissipation, favoring a rich variety of photochemical reactions or reducing photodegradation by the strong filter effect (quenching) [38].

On the other hand, nitrite ($\lambda_{\max} = 355$) and nitrate ($\lambda_{\max} = 303$) absorb light and undergo homolysis to produce $\bullet\text{OH}$ radicals and nitrogen reactive species ($\text{NO}\bullet$, $\text{NO}_2\bullet$, N_2O_3 , and N_2O_4), leading to the degradation of pollutants although $\bullet\text{OH}$ may further be scavenged by NO_2^- to form $\text{NO}_2\bullet$ [39].

3.4. Photocatalytic degradation

Although titanium dioxide (TiO_2) has been demonstrated to be an excellent catalyst and its behavior has been thoroughly reviewed in the literature, the effect of other semiconductors like ZnO is not so well known. ZnO is a very interesting wide band gap semiconductor material because of its wide band gap of 3.37 eV, large excitation binding energy of 60 MeV at room temperature, and piezoelectric properties. The band gap of this semiconductor corresponds to a radiation wavelength of around 390 nm.

As can be seen in Fig. 3, the use of ZnO strongly enhances the decomposition of all PAHs, more than 98% of the pollutant initially present in the groundwater being degraded after 2 h of illumination. The remaining percentage was lower to 12% after 10 min of treatment in all cases. Complete degradation was obtained after 50 min with the exception of B[b]F and b[k]F which require 120 and 360 min, respectively.

The results obtained for TiO_2 system show a clear improvement in the efficiency of degradation compared to photolytic tests, although they do not improve those obtained for ZnO system. After 30 minutes of exposure, the remaining percentages ranged from 8% to 36% for FI and B[a]P, respectively. After 120 minutes of illumination in the presence of TiO_2 , the remaining amounts were lower than 5% in all cases. Only B[k]F (2%) and B[ghi]P (1%) were recovered from the water after 360 min of illumination.

Total organic carbon (TOC) was measured at the beginning and the end of the photolytic and photocatalytic tests. The initial TOC value (after 15 min of homogenization) was $262 \pm 12 \mu\text{g L}^{-1}$. The mean concentrations of TOC recorded after 480 min for ZnO and TiO_2 systems were 21 and $38 \mu\text{g L}^{-1}$, respectively. For photolytic test, at the end of the experiment $158 \mu\text{g L}^{-1}$ of TOC were measured which it is indicative of a slow mineralization in absence of photocatalyst. Photodegradation of PAHs generally occurs via an oxidation reaction, leading to the formation of new photomodified compounds which are in many cases more water soluble and toxic than their parent compounds. Quinones, ketones and alcohols are major intermediates in the photooxidation of PAHs [40].

The pH of the solution appears to play and important role in the photocatalytic degradation of organic wastes because it influences the surface charge of the semiconductor, thereby affecting interfacial electron transfer and the photoredox process. In the present case, the experiments were carried out at an initial pH of around 8.1. As photodegradation progressed, there was a weak decrease in pH (about 0.3–0.4 units) due to the production of sulfuric acid. As regards temperature, because of photonic activation, photocatalytic systems do not require heating and operate at room temperature. In our study, temperature was maintained at $25 \pm 2^\circ\text{C}$.

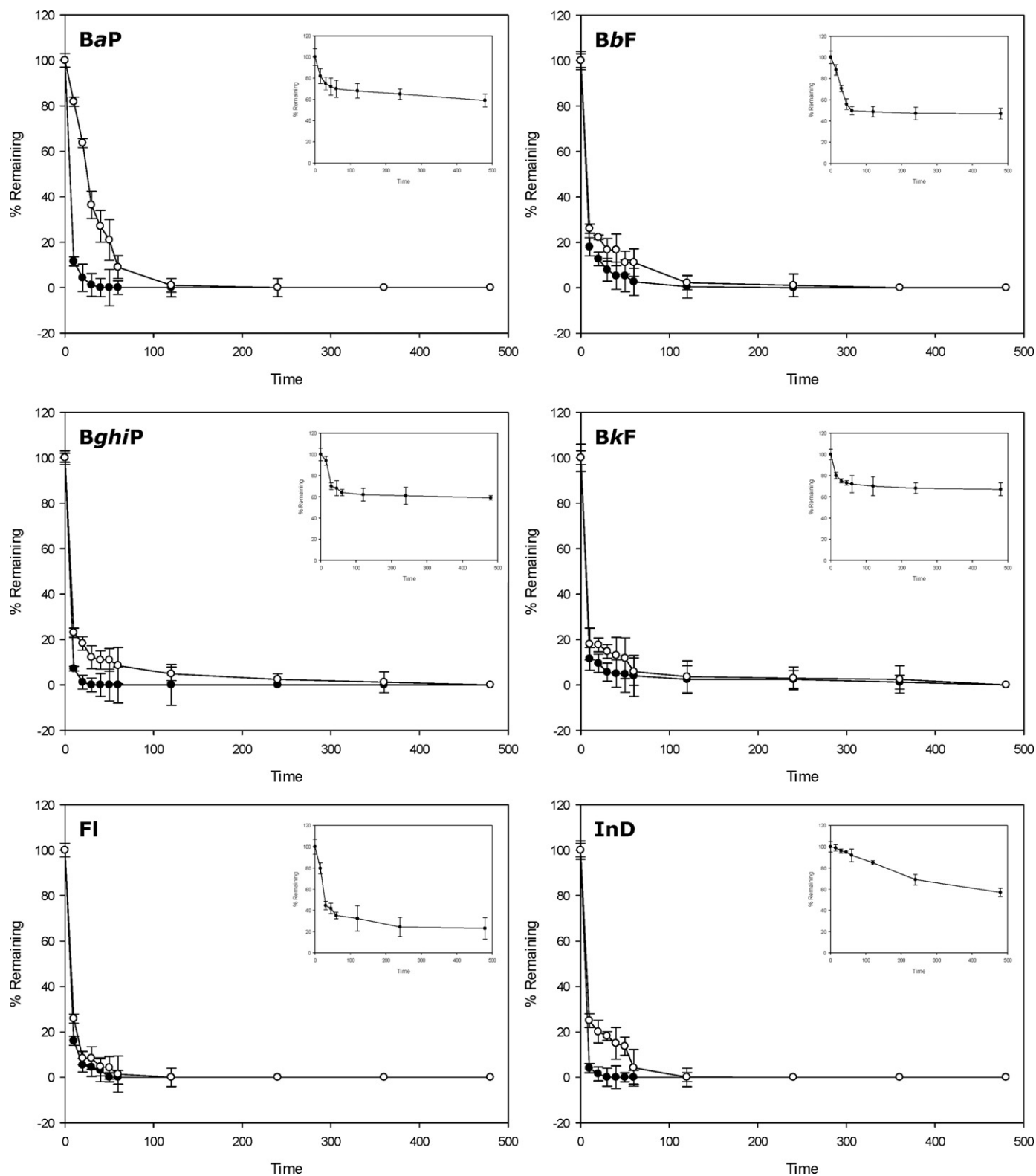


Fig. 3. Disappearance kinetics of the studied PAHs by photocatalysis with ZnO (●) and TiO₂ (○) during the photoperiod. Error bars denote standard deviation. Photolysis results are shown in the inserted graphics.

One practical problem in using semiconductors is e^-/h^+ recombination, which can be diminished in the presence of a suitable electron acceptor. For this purpose, air was introduced in the tank at regular intervals to maintain the O₂ concentration around 4–6 mgL⁻¹. Molecular oxygen plays an important role in the

photooxidation process. The principal role of dissolved oxygen in the photodegradation process is to act as an electron sink, although some authors suggest that it can act as “inner filter” or “scavenger” because molecular oxygen has absorption bands at 185 and 254 nm [41]. However, the spectrum sunlight at earth’s surface begins

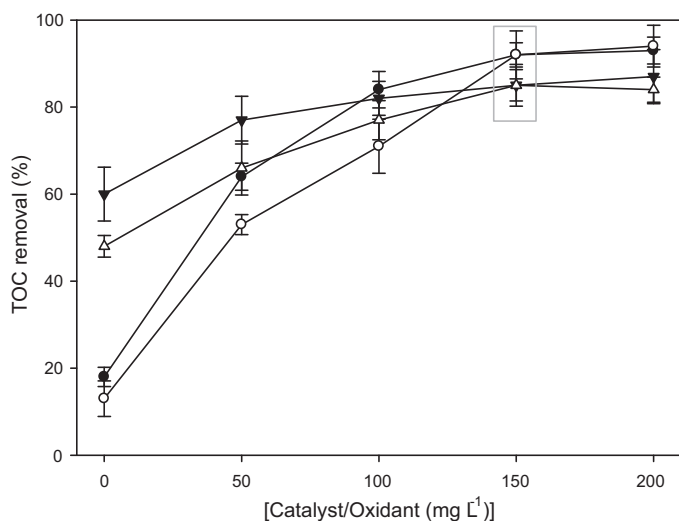


Fig. 4. Percentage of TOC removed as function of initial concentrations of ZnO, TiO₂ and Na₂S₂O₈ after 240 min. (●) Variable [ZnO], Fixed [Na₂S₂O₈] = 150 mg L⁻¹; (○) Variable [TiO₂], Fixed [Na₂S₂O₈] = 150 mg L⁻¹; (▼) Variable [Na₂S₂O₈], Fixed [ZnO] = 150 mg L⁻¹; (△) Variable [Na₂S₂O₈], Fixed [TiO₂] = 150 mg L⁻¹. Error bars denote standard deviation.

around 300 nm. Therefore, the filter effect was not important in our case.

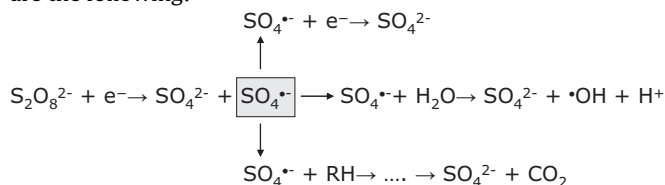
Although the results support the effectiveness of the process in the degradation of PAHs, very few studies on the photodegradation of PAHs using ZnO as catalyst have been published. Recently, Kou et al. [42] showed in their study that GaN:ZnO has excellent activity for the photodegradation of PAHs, establishing the following order of effectiveness: phenanthrene > benzo[*a*]anthracene > anthracene > acenaphthene, with complete degradation after 1, 3, 6 and 8 h, respectively. On the other hand, more papers have been published about the role of TiO₂ on the PAHs photodegradation. Thus, Dass et al. [43] analyzed the degradation of acenaphthene, anthracene, fluorene and naphthalene in aqueous suspension of TiO₂ and irradiation with UV and natural light, finding high effectiveness in the treatment due to the formation of hydroxyl and superoxide radicals. Ireland et al. [44] studied the photocatalysis of some PAHs with TiO₂, obtaining half-lives of 2.7 h in the case of anthracene and 380 h for fluoranthene. However, Sabaté et al. [45] conclude that the photolytic degradation of fluorene was more efficient than sensitized photocatalytic oxidation in the presence of TiO₂. García-Martínez et al. [46] analyzed the photodegradation of naphthalene (the most water soluble PAH) using TiO₂ (anatase) catalyst, obtaining conversion rates of 25–40% depending on the type of lamp and the tank. Wen et al. [47] studied the photocatalysis of phenanthrene (PAH of low solubility) in aqueous TiO₂ suspensions under UV light irradiation and the influence of different parameters in the photooxidation reaction concluding that the compound was completely degraded after 40 minutes without significant effect of pH or amount of photocatalyst on degradation.

3.5. Effect of catalysts and Na₂S₂O₈ concentrations

In slurry photocatalytic processes, the amount of photocatalyst and oxidant is an important parameter that can affect the degradation rates of the organic pollutants. The photomineralization rate of a pollutant is generally found to increase with catalyst concentration, reaching a limiting value at high concentration of photocatalyst. This limit depends on the geometry and working conditions of the photoreactor and applies to a given amount of catalyst in which all the particles, i.e., the whole exposed

surface, are totally illuminated; however if the catalyst concentration is very high (>2.5 g L⁻¹), turbidity impedes further penetration of light into the reactor [48,49]. For this reason, prior to the beginning of the experiments we have optimized the concentrations of semiconductor and oxidant under laboratory conditions. For this purpose, a photochemical reactor (2000 mL) equipped with a magnetic stirring bar, and 8 W low pressure mercury lamp (300–460 nm) was used. The study was carried out in a batch recirculation mode. The optimum value for both semiconductors was about 150–200 mg L⁻¹, at which concentration, more than 92% and 85% of the TOC was removed after 240 min for ZnO and TiO₂ systems, respectively (Fig. 4). Above this concentration, the suspended catalyst particles may block the passage of light and increase light scattering.

On the other hand, the addition of an electron acceptor, such as inorganic peroxide (S₂O₈²⁻) to a semiconductor suspension usually enhances the photodegradation rate of organic pollutants, since these substances capture the photogenerated electrons more efficiently than dissolved oxygen, leading to a reduction of the electron–hole recombination. Na₂S₂O₈ traps the photogenerated electron and reduces the probability of recombination with the positive hole, generating SO₄^{•-} radicals, which are also a very strong oxidizing species (reduction potential of SO₄^{•-} E° = 2.6 V), and more hydroxyl radicals [49,50]. The reactions where Na₂S₂O₈ is involved are the following:



In our experimental conditions, 150 mg L⁻¹ of Na₂S₂O₈ was found as optimal concentration for ZnO and TiO₂ systems as can be seen in Fig. 4.

3.6. Kinetics of the process

A knowledge of kinetics is required to assess the efficiency of systems used for the photooxidation of PAHs. The kinetic parameters of PAHs are shown in Tables 2 and 3 where the apparent rate constants and half-lives are listed. In all cases, the kinetics of dissipation (Fig. 3) followed an apparent first-order degradation curve, with R² ranging from 0.976 to 0.999 and 0.906 to 0.990 for ZnO and TiO₂ systems, respectively. The amount of time required for 50% of its initial PAH concentration to be degraded ranged from 2.2 to 4.6 and 5.3 to 23.1 min in aqueous suspensions of ZnO and TiO₂, respectively.

Results summarized in Tables 2 and 3 demonstrate that the biphasic model (Hoerl function) which considers an initial rapid degradation followed by a second sluggish disappearance, produce a much better fitting to the experimental data than the usual monophasic model (first-order). The function is inherently more flexible than the first-order equation because has more parameters. An additional advantage of the Hoerl function, in contrast to the biexponential, is that the Hoerl function can be used with standard linear regression rather than non-linear methods. In all cases the “*c*” values ranging from 0.07 to 0.18 are smaller than zero in the case of ZnO system and indicate a biphasic pattern. This means that the slope (or loss of PAHs in this case) is faster soon after application and slower long after application. For TiO₂ system, the “*c*” values are also smaller than zero, with the exception of B[*a*]P. The values of R², the coefficient of multiple determination obtained from the Hoerl equation were higher than 0.998 (ZnO) and 0.993 (TiO₂) for all the PAHs, and the standard error of estimation (S_{y/x}) was markedly lower than in the first-order model. A model with more

Table 2
Kinetic parameters of the PAHs by photocatalysis with ZnO during the photoperiod.

PAHs	$C_t = C_0 \cdot e^{-kt}$					$C_t = a \cdot e^{bt} \cdot t^c$					
	$S_{y/x}^a$	R_0	K (min ⁻¹)	Adj. R^2	$t_{1/2}^b$	$S_{y/x}^a$	a	b	c	Adj. R^2	DT ₅₀ ^b
[BaP]	1.03	99.9	0.21	0.998	3.3	0.23	40.0	0.10	-0.09	0.999	1.5
[BbF]	4.50	99.4	0.15	0.976	4.6	0.53	32.9	0.03	-0.12	0.999	0.9
[BghiP]	0.22	100.0	0.26	0.999	2.7	0.07	51.2	0.18	-0.07	1.000	1.5
[BkF]	4.32	99.8	0.20	0.978	3.5	1.11	18.9	0.01	-0.18	0.998	1.0
[Fl]	1.88	99.9	0.17	0.996	4.1	0.98	40.4	0.07	-0.10	0.999	1.0
[InD]	0.45	103.3	0.32	0.999	2.2	0.16	17.9	0.11	-0.18	1.000	0.9

^a Standard deviation of the fitting (standard error of estimate).^b Time in min.**Table 3**
Kinetic parameters of the PAHs by photocatalysis with TiO₂ during the photoperiod.

PAHs	$C_t = C_0 \cdot e^{-kt}$					$C_t = a \cdot e^{bt} \cdot t^c$					
	$S_{y/x}^a$	R_0	K (min ⁻¹)	Adj. R^2	$t_{1/2}^b$	$S_{y/x}^a$	a	b	c	Adj. R^2	DT ₅₀ ^b
[BaP]	4.55	105.3	0.03	0.984	23.1	2.92	118.7	0.04	0.01	0.993	23.7
[BbF]	9.07	95.4	0.08	0.898	8.7	1.18	39.4	0.02	-0.10	0.998	2.0
[BghiP]	7.71	97.9	0.11	0.926	6.3	1.39	33.0	0.01	-0.12	0.998	2.0
[BkF]	8.81	98.3	0.13	0.902	5.3	1.86	29.4	0.01	-0.13	0.997	1.5
[Fl]	2.96	99.6	0.13	0.990	5.3	1.92	52.2	0.06	-0.07	0.996	3.0
[InD]	8.82	96.9	0.09	0.906	7.7	2.36	40.3	0.02	-0.10	0.993	2.0

^a Standard deviation of the fitting (standard error of estimate).^b Time in min.**Table 4**
Economic assessment for water treatment by heterogeneous (ZnO and TiO₂) photocatalysis.

Costs	ZnO	TiO ₂
I. Collector (€ year ⁻¹)		2969.42
II. Engineering (€ year ⁻¹)		200.00
III. Operation and maintenance (€ year ⁻¹)	2.5% I + II	79.24
IV. Consumables (€ year ⁻¹)		
	Unit price	
	Na ₂ S ₂ O ₈ (€/kg)	3
	ZnO (€/kg)	617.01
	TiO ₂ (€/kg)	740.41
		168.13
	Total reagents	1357.42
V. Service (€ year ⁻¹)		
	Unit price	
	Water € L ⁻¹	0.001
	Electricity €(kW h ⁻¹)	0.16
	Total service	26.40
	Total I + II + III + IV + V	397.12
		423.52
VI. Overheads (€ year ⁻¹)	10% I + II + III + IV + V	
		5029.60
		3952.40
		502.96
		395.24
	Total I + II + III + IV + V + VI	5532.55
	t_{90}	12.78
	TC (m ³ year ⁻¹)	70.34
		2056.69
		373.63
Treatment cost (€/m ³)		2.69
		11.64

terms may appear to have a better fit (higher R^2) simply because it has more parameters to be adjusted (or less degrees of freedom). In order to compare the quality of the different proposed models and balance their different degrees of freedom it is important to use the Adjusted R^2 , a useful index for comparing the explanatory power of models with different numbers of predictors. The Adj- R^2 will increase only if the addition of a new parameter improves the model more than would be expected by chance. The closer (Adj- R^2) approaches 1, the better the model fits the data. By use of the Hoerl function better Adj- R^2 were obtained in all cases. The DT₅₀ values, graphically estimated agree with the experimental data.

3.7. Cost estimate for water treatment

A comparison of the treatment cost of the ZnO system with regard to the cost of the TiO₂ system under the same experimental conditions is showed in Table 4. Bearing in mind that the SE of Spain receives about 3000 h of sunlight per year and that the average of useful minutes of the pilot plant (UM) is 480 min day⁻¹, the

treatment capacity (TC) of our system was calculated according to the following equation:

$$TC (\text{L/year}) = \frac{UM \times V \times 365}{t_{90}} \quad (5)$$

where V is the volume of water treated (150 L) and t_{90} is the amount of time required for 90% of the initial pollutant concentration to dissipate and was calculated according to the following equation:

$$t_{90} = \frac{\ln 10}{k} = \frac{2.303}{k} \quad (6)$$

where k is the rate constant. In our case, the selected t_{90} was the t_{90} of the PAH with lower value of k.

The treatment cost was estimated to be 2.69 €/m³ for the ZnO/Na₂S₂O₈ system and 11.64 €/m³ for the TiO₂/Na₂S₂O₈ system. The significant differences found in cost between both treatments are attributed to the high reaction rate observed for the studied compounds by treatment with ZnO.

4. Conclusions

Although PAHs can be found in leachates the mobility of these persistent organic pollutants in soil is very small, since most of the compound applied is retained in the top fraction of soil (0–10 cm). Only, a small percentage (<1%) was recovered from the bottom fraction (10–20 cm).

The use of solar photocatalysis in presence of ZnO and TiO₂ as photocatalysts constitutes a very effective method for the removal of the selected PAHs in groundwater. A synergistic effect was especially observed with the addition of the oxidant (Na₂S₂O₈) into illuminated ZnO suspensions by enhancing the efficiency of the process.

Bearing in mind the groundwater pollution problems, photocatalysis offers a good and economical technology as substitute to other conventional methods for water remediation by using a renewable source of energy, inexhaustible and pollution-free, like sunlight mainly in some Mediterranean areas as SE of Spain receiving more than 3000 h of sunlight per year.

References

- [1] J. Stellman, M. McCann, Encyclopedia of Occupational Health and Safety, vol. III, International Labour Office-Geneva, 1998.
- [2] S.W. Moore, S. Ramamorthy, Organic chemicals in natural waters, in: R.S. Desanto (Ed.), Applied Monitoring and Impact Assessment, Springer-Verlag, New York, 1984.
- [3] IARC. International Agency for Research on Cancer, Monographs on the Evaluation of the Carcinogenic Risk of Chemicals to Humans. Overall Evaluation of Carcinogenicity: An Updating of IAPC Monographs, vols. 1–42, Suppl. 7, International Agency for Research on Cancer, Lyon, France, 1987.
- [4] S. Baek, M. Goldstone, P. Kirk, J. Lester, R. Perry, Phase distribution and particle size dependency of polycyclic aromatic hydrocarbons in the urban atmosphere, *Chemosphere* 22 (1991) 503–520.
- [5] NRC, Polycyclic Aromatic Hydrocarbons: Evaluation of Sources and Effects, National Research Council, National Academy Press, ES/1-ES/7, Washington, D.C., 1983.
- [6] C. Jiang, R. Alexander, R. Kagi, A. Murray, Origin of perylene in ancient sediments and its geological significance, *Org. Geochem.* 31 (2000) 1545–1559.
- [7] G. Brun, O. Vaidya, M. Léger, Atmospheric deposition of polycyclic aromatic hydrocarbons to Atlantic, Canada: geographic and temporal distributions and trends 1980–2001, *Environ. Sci. Technol.* 38 (2004) 1941–1948.
- [8] J. Clemons, L. Allan, C. Marvin, Z. Wu, B. McCarry, D. Bryant, Evidence of estrogen and TCDD-like activities in crude and fractionated extracts of PM10 air particulate material using in vitro gene expression assays, *Environ. Sci. Technol.* 32 (2004) 1853–1860.
- [9] X. Liu, G. Zhang, K. Jones, X. Li, X. Peng, S. Qi, Compositional fractionation of polycyclic aromatic hydrocarbons (PAHs) in mosses (*Hypnum plumaeformae* WILS) from the northern slope of Nanling Mountains, South China, *Atmos. Environ.* 39 (2005) 5490–5499.
- [10] T. Ramdahl, I. Alfheim, A. Bjorseth, Nitrated polycyclic aromatic-hydrocarbons in urban air particles, *Environ. Sci. Technol.* 16 (1982) 861–865.
- [11] D.J. Freemann, C.R. Cattell, Woodburning as a source of atmospheric polycyclic aromatic hydrocarbons, *Environ. Sci. Technol.* 24 (1990) 1581–1585.
- [12] Y.L. Tan, J.F. Quanci, R.D. Borys, Polycyclic aromatic hydrocarbons in smoke particles from wood and duff burning, *Atmos. Environ.* 26 (1992) 1177–1181.
- [13] R. Wahaab, M. Badawy, Water quality and sources of pollution in Egypt, *Int. J. Biomed. Environ. Sci.* 17 (2004) 87–100.
- [14] J. Helfrish, D. Armstrong, Polycyclic aromatic hydrocarbons in sediments of southern basin of Lake Michigan, *J. Great Lake Res.* 12 (1986) 1992–1998.
- [15] Z. Shi, S. Tao, B. Pan, W. Fan, X. He, Q. Zuo, S. Wu, B. Li, J. Cao, W. Liu, F. Xu, X. Wang, W. Shen, P. Wong, Contamination of rivers in Tianjin, China by polycyclic aromatic hydrocarbons, *Environ. Pollut.* 134 (2005) 97–111.
- [16] J.C. Chuang, G.A. Mack, M.R. Kuhlman, Polycyclic aromatic hydrocarbons and their derivatives in indoor and outdoor air in an eight-home study, *Atmos. Environ. B-Urb.* 25 (1991) 369–380.
- [17] D. Hoffmann, I. Hoffmann, Tobacco smoke as a respiratory carcinogen, in: A. Hirsch, M. Goldberg, J.P. Martin (Eds.), Prevention of Respiratory Diseases, Marcel Dekker Inc., New York, 1993, pp. 497–532.
- [18] J.L. Mumford, R.W. Williams, D.B. Walsh, Indoor air pollutants from unvented kerosene heater emissions in mobile homes: Studies on particles, semivolatile organics, carbon monoxide, and mutagenicity, *Environ. Sci. Technol.* 25 (1991) 1732–1738.
- [19] G.W. Traynor, M.G. Apte, H.A. Sokol, Selected organic pollutant emissions from unvented kerosene space heaters, *Environ. Sci. Technol.* 24 (1990) 1265–1270.
- [20] E. Lipiatou, J. Tolosa, R. Simo, I. Bouloubassi, J. Dachs, S. Marti, M.A. Sicre, J.M. Bayona, J.O. Grimalt, A. Saliot, J.J. Albaiges, Mass budget and dynamics of polycyclic aromatic hydrocarbons in the Mediterranean Sea, *Top. Stud. Oceanogr.* 44 (1997) 881–905.
- [21] U. Zoller, Groundwater contamination by detergents and polycyclic aromatic hydrocarbons – a global problem of organic contaminants: is the solution locally specific, *Water Sci. Technol.* 27 (1993) 187–194.
- [22] S. Menzie, B. Potocki, J. Santodonato, Exposure to carcinogenic PAHs in the environment, *Environ. Sci. Technol.* 14 (1992) 1524–1528.
- [23] M. Bomboi, A. Hernandez, Hydrocarbons in urban runoff: their contribution to the wastewaters, *Water Res.* 25 (1991) 557–565.
- [24] WFD, Directive 2000/60/EC of the European Parliament and of the Council of 23 October 2000 establishing a framework for Community action in the field of water policy, *Off. J. Eur. Commun. L327* (2000) 1–69.
- [25] GWD, Directive 2006/118/EC of the European Parliament and of the Council of 12 December 2006 on the protection of groundwater against pollution and deterioration, *Off. J. Eur. Commun. L372* (2006) 19–31.
- [26] K. Kveseth, B. Sortland, T. Bokn, Aromatic hydrocarbons in sewage mussels and tap water, *Chemosphere* 11 (1982) 623–639.
- [27] C.P. Huang, C. Dong, Z. Tang, Advanced chemical oxidation: Its present role and potential future in hazardous waste treatment, *Waste Manage.* 13 (1993) 361–377.
- [28] US EPA, Estimation Programs Interface Suite™ for Microsoft® Windows, v4.1, United States Environmental Protection Agency, Washington, D.C., 2011.
- [29] ISSS-ISRIC-FAO, World Reference Base for Soil Resources. World Soil Resources Report 84, FAO UN, Rome, 1998, pp. 88.
- [30] OECD, Organisation for Economic Cooperation and Development. Guidelines for Testing of Chemicals, No. 312, Leaching in Soil Columns, Paris, 2007.
- [31] A.E. Hoerl, Fitting curves to data, in: J.H. Perry (Ed.), *Chemical Business Handbook*, McGraw-Hill, New York, 1954, pp. 55–57.
- [32] M. Pérez-Moya, M. Graells, P. Buenestado, H.D. Mansilla, A comparative study on the empirical modeling of Photo-Fenton process performance, *Appl. Catal. B: Environ.* 84 (2008) 313–323.
- [33] C. Daniel, F. Woods, *Fitting Equations to Data*, 2nd ed., John Wiley & Sons, New York, 1980.
- [34] V. Sit, M. Poulin-Costello, Catalogue of Curves for Curve Fitting. Biometrics Information, Handbook, 4, British Columbia Ministry of Forests, Victoria, BC, 1994.
- [35] A.M. Rivera-Figueroa, K.A. Ramazan, B.J. Finlayson-Pitts, Fluorescence, absorption and excitation spectra of polycyclic aromatic hydrocarbons as a tool for quantitative analysis, *J. Chem. Educ.* 81 (2004) 242–245.
- [36] M.P. Fasnacht, M.P. Blough, Mechanisms of the aqueous photodegradation of polycyclic aromatic hydrocarbons, *Environ. Sci. Technol.* 37 (2003) 5767–5772.
- [37] P.P. Vaughan, M.P. Blough, Photochemical formation of hydroxyl radical by constituents of natural waters, *Environ. Sci. Technol.* 32 (1998) 2947–2953.
- [38] M.P. Fasnacht, M.P. Blough, Aqueous photodegradation of polycyclic aromatic hydrocarbons, *Environ. Sci. Technol.* 36 (2002) 4364–4369.
- [39] J. Mack, J.R. Bolton, Photochemistry of nitrite and nitrate in aqueous solution: a review, *J. Photochem. Photobiol. A-Chem.* 128 (1999) 1–13.
- [40] A. Kot-Wasik, D. Dabrowska, J. Namiesnik, Photodegradation and biodegradation study of benzo(a)pyrene in different liquid media, *J. Photochem. Photobiol. A-Chem.* 168 (2004) 109–115.
- [41] H. Shirayama, Y. Tobezo, S. Taguchi, Photodegradation of chlorinated hydrocarbons in the presence and absence of dissolved oxygen in water, *Water Res.* 35 (2001) 1941–1950.
- [42] J. Kou, Z. Li, Y. Guo, J. Gao, M. Yang, Z. Zou, Photocatalytic degradation of polycyclic aromatic hydrocarbons in GaN:ZnO solid solution-assisted process: direct hole oxidation mechanism, *J. Mol. Catal. A: Chem.* 325 (2010) 48–54.
- [43] S. Dass, M. Muneer, K.R. Gopidas, Photocatalytic degradation of wastewater pollutants. Titanium-dioxide-mediated oxidation of polynuclear aromatic hydrocarbons, *J. Photochem. Photobiol. A: Chem.* 77 (1994) 83–88.
- [44] J.C. Ireland, B. Dávila, H. Moreno, S.K. Fink, S. Tassos, Heterogeneous photocatalytic decomposition of polyaromatic hydrocarbons over titanium dioxide, *Chemosphere* 30 (1995) 956–984.
- [45] J. Sabaté, J.M. Bayona, A.M. Solanas, Photolysis of PAHs in aqueous phase by UV irradiation, *Chemosphere* 44 (2001) 119–124.
- [46] M.J. García-Martínez, L. Canoira, G. Blázquez, I. Da Riva, R. Alcántara, J.F. Llamas, Continuous photodegradation of naphthalene in water catalyzed by TiO₂ supported on glass Raschig rings, *Chem. Eng. J.* 110 (2005) 123–128.
- [47] S. Wen, J. Zhao, G. Sheng, J. Fu, P. Peng, Photocatalytic reactions of phenanthrene at TiO₂/water interfaces, *Chemosphere* 46 (2002) 871–877.
- [48] J.M. Herrmann, Heterogeneous photocatalysis: state of the art and present applications, *Top. Catal.* 34 (2005) 49–65.
- [49] S. Malato, P. Fernández-Ibáñez, M.I. Maldonado, J. Blanco, W. Gernjak, Decontamination and disinfection of water by solar photocatalysis: recent overview and trends, *Catal. Today* 147 (2009) 1–59.
- [50] S. Ahmed, M.G. Rasul, R. Brown, M.A. Hashib, Influence of parameters on the heterogeneous photocatalytic degradation of pesticides and phenolic contaminants in wastewater: a short review, *J. Environ. Manage.* 92 (2011) 311–330.